Research Article

Quantum Chemical Calculations on the Geometrical, Spectroscopic (FTIR, FT-Raman) analysis of 1,4-dibromo-2,5-difluorobenzene for Pharmaceutical Application

S. Jeyavijayan*, B. Vijitha, I. Vigneshwari
Department of Physics, Kalasalingam University, Krishnankoil, Tamilnadu-626 126, India.
***Corresponding author's E-mail:** sjeyavijayan@gmail.com

Received: 21-11-2017; **Revised:** 28-12-2017; **Accepted:** 15-01-2018.

ABSTRACT

Benzene derivatives have been widely used to manufacture therapeutic chemicals, dyes, artificial leather and detergent products. In this work, the experimental FTIR (4000–400 cm^{-1}) and FT-Raman spectra (3500-50 cm-1) of 1,4-dibromo-2,5-difluorobenzene (BFB) in solid phase have been recorded. The theoretical vibrational frequencies and optimized geometric parameters have been calculated by using density functional theory (DFT) quantum chemical method with 6-311++G (d, p) basis set. The assignments of the vibrational frequencies have been done by total energy distribution (TED) analysis. The theoretical optimized geometric parameters and vibrational frequencies have been found to be in good agreement with the corresponding experimental data, and with the results in the literature. The highest occupied molecular orbital (HOMO) energy, the lowest unoccupied molecular orbital (LUMO) energy and the other related molecular energies of the compound have been investigated using the same theoretical calculation. Molecular electrostatic potential (MEP) results predicted that the bromine and fluorine atoms of BFB to be the most reactive site for both electrophilic and nucleophilic attack. The NBO result reflects the charge transfer from fluorine and bromine atoms to benzene ring, due to the orbital overlap of n3(F8) → π*(C1-C2) and n3(Br7) → π*(C1-C2).

Keywords: FTIR, FT-Raman, DFT calculations, 1, 4-dibromo-2, 5-difluorobenzene, NBO.

INTRODUCTION

Benzene is a natural part of crude oil, gasoline, and cigarette smoke[1,2]. It is used to make some types of rubbers, lubricants, dyes, detergents, drugs, and pesticides. Benzene derivatives have been widely used to manufacture therapeutic chemicals, dyes, artificial leather and detergent products. Further, the fluoro benzene derivatives are used to control carbon content in steel manufacturing. They are also an intermediate for pharmaceuticals, pesticides and other organic compounds. When substituted benzene molecules undergo electrophilic substitution reactions, substituents on a benzene ring can influence the reactivity. The inclusion of substituents in benzene leads to the variation of charge distribution in the molecule, and consequently affects the structural, electronic and vibrational parameters. Because of these versatile behaviors of benzene, Mahadevan *et al.*[3], have extensively studied the FTIR and FT-Raman, UV spectroscopic investigation of 1-bromo-3-fluorobenzene using DFT (B3LYP, B3PW91 and MPW91PW91) calculations. Kolesnikova *et al.*[4] have investigated the molecular structure and conformation of 1,3,5-tris(trifluoromethyl)benzene by gas-phase electron diffraction and quantum chemical calculations. The spectroscopic study of human hemoglobin structural and functional alterations and heme degradation upon interaction with benzene was investigated by Hosseinzadeh *et al.*[5]. More recently, Vennila *et al.*[6] investigated a complete computational and spectroscopic study of 2-bromo-1, 4-dichlorobenzene. Literature survey reveals that to the best of our knowledge no density functional theory (DFT) with 6-311++G(d,p) basis set calculations of 1,4-dibromo-2,5-difluorobenzene (BFB) have been reported so far. Therefore, an attempt has been made in the present work to study the detailed theoretical (DFT) and experimental (FTIR and FT-Raman) investigation of the vibrational spectra of BFB.

EXPERIMENTAL DETAILS

The fine sample of BFB was purchased from Lancaster chemical company, UK and it was used as such without any further purification to record FTIR and FT-Raman spectra. The FTIR spectra of the title compound was recorded in the region 4000-400 cm^{-1} at a resolution of ±1cm^{-1} using BRUCKER IFS 66V model FTIR spectrometer equipped with an MCT detector, a KBr beam splitter and globar source.

The FT-Raman spectrum of BFB was recorded using 1064 nm line of Nd: YAG laser as excitation wavelength in the Stokes region (3500-50 cm^{-1}) on a BRUKER IFS-66V model interferometer equipped with an FRA-106 FT-Raman accessory operating at 200mW power. The calibrated wave numbers are expected to be accurate within ±1cm^{-1}.

Computational Details

For meeting the requirements of both accuracy and computing economy, theoretical methods and basis sets should be considered. DFT has proved to be extremely useful in treating electronic structure of molecules. The DFT calculations were carried out for BFB with GAUSSIAN 09W program package[7] using the Becke's three parameter hybrids functional combined with the Lee-Yang-Parr correlation (B3LYP) functional[8,9] with standard 6-311++G(d, p) basis set. All the parameters were allowed

to relax and all the calculations converged to an optimized geometry which corresponds to a true minimum, as revealed by the lack of imaginary values in the wave number calculations. The Cartesian representation of the theoretical force constants have been computed at the fully optimized geometry. Transformation of force field and calculation of the total energy distribution (TED) were done on a PC with the MOLVIB program (version V7.0-G77) written by Sundius[10]. The systematic comparison of the results from DFT theory with results of experiments has shown that the method using B3LYP functional is the most promising in providing correct vibrational wave numbers. The redistribution of electron density (ED) in various bonding and antibonding orbital and hyper conjucative interaction energies $E^{(2)}$ have been calculated by natural bond orbital analysis with B3LYP/6-311++G(d,p) method to give clear evidence of stabilization originating from the hyper conjugation of various intermolecular interactions. The HOMO and LUMO analyses have been used to elucidate information regarding charge transfer within the molecule.

RESULTS AND DISCUSSION

Molecular geometry

The optimized molecular structure of BFB along with numbering of atoms is shown in Fig. 1. The most optimized structural parameters (bond length and bond angle) calculated by DFT/B3LYP with 6-311++G (d, p) basis set are compared with X-ray diffraction experimental data[11, 12] and represented in Table 1. The calculated geometric parameters can be used as foundation to calculate the other parameters for the compound.

Table 1: Optimized geometrical parameters of 1,4-dibromo-2,5-difluorobenzene obtained by B3LYP/6-311++G(d,p) method.

Bond length	Value (Å)		Bond angle	Value (°)		Dihedral Angle	Value (°)
	B3LYP/ 6-311++G (d, p)	Expt values[a]		B3LYP/ 6-311++G (d, p)	Expt values[a]		B3LYP/ 6-311++G (d, p)
C1-C2	1.3922	1.402	C2-C1-C6	119.1008	121.8	C6-C1-C2-C3	0.0
C1-C6	1.3918	1.386	C2-C1-Br7	120.4162	121.5	C6-C1-C2-F8	180.0
C1-Br7	1.8991	1.889	C6-C1-Br7	120.483	121.5	Br7-C1-C2-C3	180.0
C2-C3	1.3865	1.386	C1-C2-C3	121.3882	121.8	Br7-C1-C2-F8	0.0
C2-F8	1.3438	1.355	C1-C2-F8	120.1555	118.3	C2-C1-C6-C5	0.0
C3-C4	1.3918	1.386	C3-C2-F8	118.4563	118.3	C2-C1-C6-H12	180.0
C3-H9	1.0818	1.073	C2-C3-C4	119.511	121.1	Br7-C1-C6-C5	180.0
C4-C5	1.3922	1.386	C2-C3-H9	119.3135	120.9	Br7-C1-C6-H12	0.0
C4-Br10	1.8991	1.899	C4-C3-H9	121.1755	121.0	C1-C2-C3-C4	0.0
C5-C6	1.3865	1.386	C3-C4-C5	119.1008	121.8	C1-C2-C3-H9	180.0
C5-F11	1.3438	1.355	C3-C4-Br10	120.483	121.5	F8-C2-C3-C4	180.0
C6-H12	1.0818	1.073	C5-C4-Br10	120.4162	121.5	F8-C2-C3-H9	0.0
			C4-C5-C6	121.3882	121.8	C2-C3-C4-C5	0.0
			C4-C5-F11	120.1555	118.7	C2-C3-C4-Br10	180.0
			C6-C5-F11	118.4563	118.1	H9-C3-C4-C5	180.0
			C1-C6-C5	119.511	121.1	H9-C3-C4-Br10	0.0
			C1-C6-H12	121.1755	119.5	C3-C4-C5-C6	0.0
			C5-C6-H12	119.3135	119.4	C3-C4-C5-F11	180.0
						Br10-C4-C5-C6	180.0
						Br10-C4-C5-F11	0.0
						C4-C5-C6-C1	0.0
						C4-C5-C6-H12	180.0
						F11-C5-C6-C1	180.0
						F11-C5-C6-H12	0.0

[a]Experimental values are taken Ref. 11, 12.

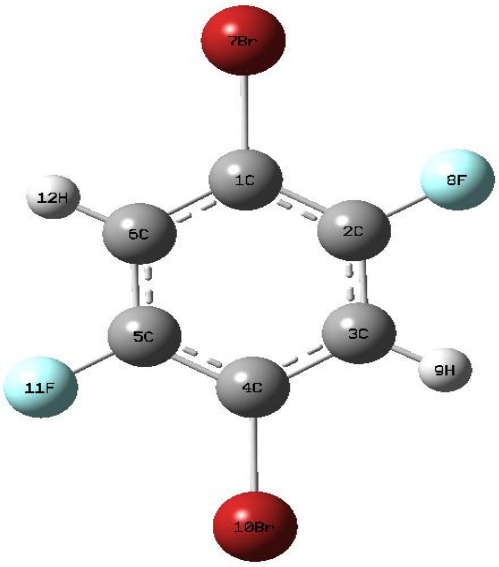

Figure 1: Molecular structure of 1, 4-dibromo-2, 5-difluorobenzene.

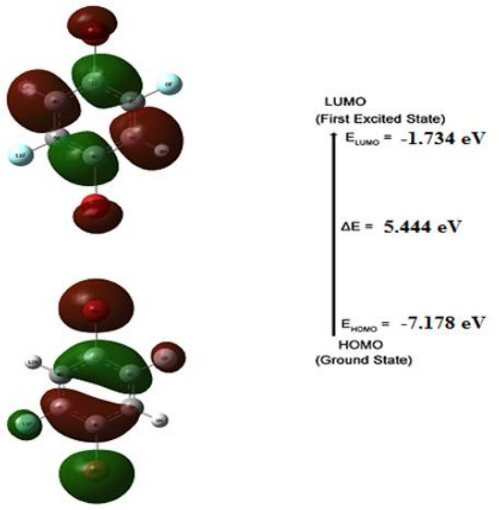

Figure 2: Frontier molecular orbital for 1,4-dibromo-2,5-difluorobenzene.

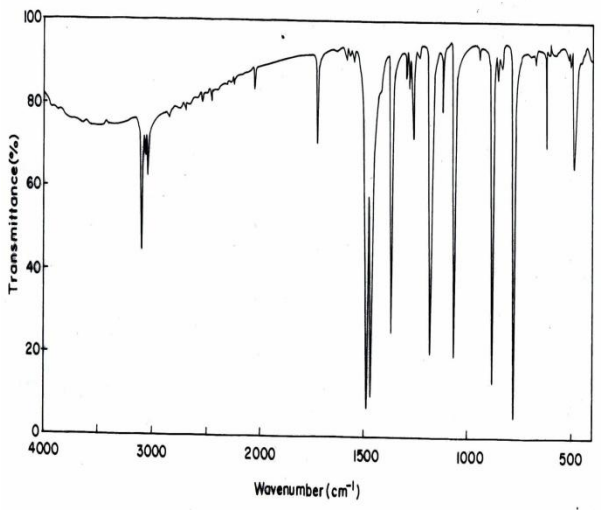

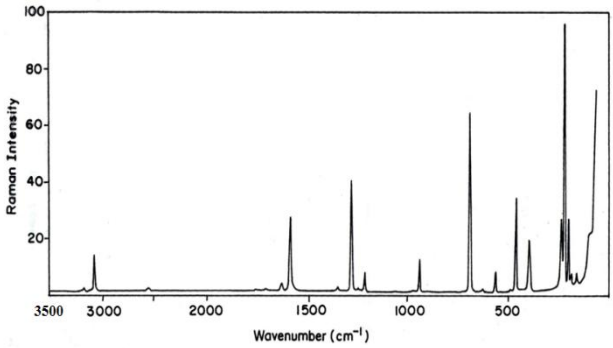

Figure 3: FTIR and FT-Raman spectra of 1,4-dibromo-2,5-difluorobenzene.

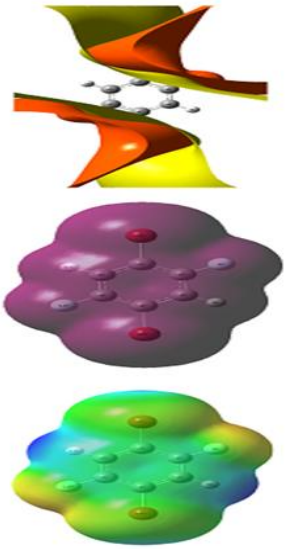

Figure 4: (a) Electrostatic potential (ESP); (b) electron density (ED) and (c) the molecular electrostatic potential (MEP) map for 1, 4-dibromo-2,5-difluorobenzene.

The optimized molecular structure of BFB reveals that the para-substituted fluorine and bromine atoms are in planar with the benzene ring. Inclusion of fluorine and bromine atoms known for its strong electron-withdrawing nature, in para position, is expected to increase a contribution of the resonance structure, in which the electronic charge is concentrated at this site. This is the reason for the increase in bond lengths of C1-Br7 (1.8991 Å) and C4-Br10 (1.8991 Å). The carbon atoms are bonded to the hydrogen atoms with an σ-bond in benzene and the substitution of fluorine and bromine atoms for hydrogen reduces the electron density at the ring carbon atom. The ring carbon atoms in substituted benzenes exerts a larger attraction on the valence electron cloud of the hydrogen atom resulting in an increase in the C-H force constants and a decrease in the corresponding bond length. The benzene ring appears to be a little distorted because of the halogen atoms as seen from the bond angles calculated. For fluorine atoms at first and fourth position of the benzene ring, the bond angles C2–C1–C6, C3–C4–C5 are calculated as 119.1° and the bond angles C1–C2–C3, C4–C5–C6 are calculated as 121.38° for

bromine atoms at second and fifth position of the benzene ring. They are differing from the typical hexagonal angle of 120°. It can be seen that there are some deviations between the computed geometrical parameters and related XRD data, and these differences are probably due to the fact that the theoretically calculated result is obtained from isolated molecule in gaseous phase while the experimental results are from molecule in solid state.

Thermodynamic properties

The values of some thermodynamic parameters (such as zero point vibrational energy, thermal energy, specific heat capacity, rotational constants and entropy) of BFB by DFT/B3LYP with 6-311++G (d, p) basis set are listed in Table 2. The global minimum energy obtained for structure optimization of BFB using DFT/B3LYP with 6-311++G (d, p) basis sets is -5577.92011704 Hartrees. Dipolemoment reflects the molecular charge distribution and is known as a vector in three dimensions. The existence of a dipolemoment is the difference between polar and non-polar bonds. Dipolemoments are strictly determined for neutral molecules. Its value depends on the choice of origin and molecular orientation for charged systems. In the present study, the molecule possesses zero dipolemoment due to its symmetrical structure. In BFB, atoms that have similar electronegativity values tend to form chemical bonds with zero dipole moment. The variation in zero-point vibrational energies (ZPVEs) seems to be significant. The total energy and the change in the total entropy of the title compound at room temperature are also presented. All the thermodynamic data provide helpful information for the further study on the BFB. According to relationships of thermodynamic functions, one can compute other thermodynamic energies and estimate directions of chemical reactions from the second law of thermodynamics in thermochemical field[13].

Table 2: The thermodynamic parameters of 1, 4-dibromo-2, 5-difluorobenzene calculated at the B3LYP/6-311++G (d,p) method.

Parameters	Method/Basis set
	B3LYP/6-311++G(d,p)
Optimized global minimum Energy (Hartrees)	-5577.92011704
Total energy(thermal), E_{total} (kcal mol^{-1})	45.370
Heat capacity, C_v (cal mol^{-1} k^{-1})	31.590
Entropy, S (cal mol^{-1} k^{-1})	
Total	96.468
Translational	42.677
Rotational	30.934
Vibrational	22.856
Vibrational energy, E_{vib} (kcal mol^{-1})	43.593
Zero point vibrational energy, (kcal mol^{-1})	39.75057
Rotational constants (GHz)	
A	1.78922
B	0.27075
C	0.23517

HOMO, LUMO analysis

Electron excitation from the highest occupied molecular orbital (HOMO) to the lowest unoccupied molecular orbital (LUMO) explains the electronic absorption corresponds to the transition from the ground to the first excited state. In BFB, the LUMO of π nature, (i.e. benzene ring) is delocalized over the whole C-C bond and the HOMO is located over fluorine and bromine atoms. Therefore, the HOMO → LUMO transition implies an electron density transfer to C-C bond of the benzene ring from fluorine and bromine atoms. Moreover, these three orbitals significantly overlap in the para position of the benzene ring for BFB. The atomic orbital compositions of the frontier molecular orbital and the HOMO–LUMO energy gap of BFB was calculated at the B3LYP/6-311++G (d, p) level are shown in Fig. 2. The HOMO-LUMO energy gap for BFB is found to be 5.444 eV. The LUMO as an electron acceptor represents the ability to obtain an electron, and HOMO represents the ability to donate an electron[14]. Moreover, a lower HOMO–LUMO energy gap explains the fact that ultimate charge transfer interaction is taking place within the molecule which reflects the chemical activity of the molecule.

Vibrational spectra

From the structural point of view the molecule is assumed to have C_{2h} point group symmetry. The molecule consists of 12 atoms and expected to have 30 normal modes of vibrations. The observed FTIR and FT-Raman spectra of BFB at DFT-B3LYP level using 6-311++G (d, p) basis set are shown in Fig. 3. The detailed vibrational assignment of fundamental modes of BFB along with the calculated IR and Raman intensities and normal mode descriptions (characterised by TED) are reported in Table 3. Form the Table 3, it can be seen that for the title molecule due to its symmetric structure, the strongest band in the Raman

spectrum is weak in the IR spectrum and vice-versa. The calculated vibrational intensities also reflect the same for the title molecule.

The calculated harmonic force constants and wavenumbers are usually higher than the corresponding experimental quantities because of the combination of electron correlation effects and basis set deficiencies. The observed slight disagreement between theory and experiment could be a consequence of the anharmonicity and the general tendency of the quantum mechanical methods to overestimate the force constants at the exact equilibrium geometry. Therefore, in order to improve the calculated values in agreement with the experimental ones, it is necessary to scale down the calculated harmonic frequencies. A better agreement between the computed and experimental frequencies can be obtained by using scale factor[15] of 0.96 for B3LYP method. The resultant scaled frequencies are also listed in Table 3.

C-H vibrations

In the experimental spectrum, C–H stretching frequencies appear in the range 3100-3000 cm^{-1}, the C–H in-plane bending vibrations[16] in the range 1300-1000 cm^{-1} and C–H out-of-plane bending vibrations in the range 1000-750 cm^{-1}. The FTIR vibrational frequencies at 3092 and 3084 cm^{-1} are assigned to C–H stretching vibrations of BFB and show good agreement with the calculated results. The Raman counterparts of C-H vibrations are observed at 3088 cm^{-1}, which are further supported by the TED contribution of almost 100%. The IR band at 1235 cm^{-1} and Raman band at 1245 cm^{-1} are assigned to C–H in-plane vibrations of BFB. The C–H out-of-plane bending vibrations of the molecule are found at 865, 822 cm^{-1} in the FTIR spectrum. These modes show consistent agreement with the computed B3LYP results.

C-C vibrations

The C-C aromatic stretching vibrations[17] gives rise to characteristic bands in both the observed IR and Raman spectra, covering the spectral range from 1650 to 1400 cm^{-1}. Therefore, the C-C stretching vibrations of the title compound are found at 1624, 1562, 1452, 1354, 1263 cm^{-1} in FTIR and 1621, 1556, 1352, 1272 cm^{-1} in the FT-Raman spectrum and these modes are confirmed by their TED values. Most of the ring vibrational modes are affected by the substitutions in the aromatic ring of the title compound. In the present study, the bands observed at 1042, 917, 762 cm^{-1} and 922 cm^{-1} in the FTIR and Raman spectrum, respectively, have been designated to ring in-plane bending modes by careful consideration of their quantitative descriptions. The ring out-of-plane bending modes of BFB are also listed in the Table 3. The reductions in the frequencies of these modes are due to the change in force constant and the vibrations of the functional groups present in the molecule. The theoretically computed values for C-C vibrational modes by B3LYP/6-311++G(d,p) method gives excellent agreement with experimental data.

C-Br vibrations

Vibrations belonging to C–Br bonds which are formed between the ring and the halogen atoms are interesting since mixing of vibrations are possible due to the lowering of molecular symmetry and the presence of heavy atoms[18]. The assignments of C–Br vibrations have been made by comparison with halogen substituted benzene derivatives. C–Br stretching vibrations[19] appear in the lower range of frequencies i.e. 650-485 cm^{-1} and C–Br deformation occur in the region 300-140 cm^{-1}. In the present investigation, the C–Br stretching vibration of BFB is observed at 620 cm^{-1} in FTIR and 693 cm^{-1} in Raman spectrum. The C–Br deformation vibrations also agree well with the expected results.

C-F vibrations

Assignments of the C–F stretching modes are very difficult as these vibrations are strongly coupled with the other in plane bending vibrations of several modes. Normally, the C–F stretching vibrations[20] strongly coupled with the C–H in-plane bending vibrations in the mono fluorinated benzene and are observed in the region 1100-1000 cm^{-1}. The present molecule has two fluorine atoms which are placed at second and fifth position of the skeletal ring. The C–F stretching vibrations of BFB are observed at 1205 and 1156 cm^{-1} in the IR spectrum. Generally, the C–F in-plane bending[21] and out-of-plane bending wavenumbers are assigned at 402 cm^{-1} and 377 cm^{-1} in Raman spectra, respectively. In the present case, the C–F in-plane bending are assigned at 210, 202 cm^{-1} in Raman spectrum. The frequencies of the C–F out-of-plane bending vibration of BFB are also listed in Table 3.

NBO analysis

In order to understand various second-order interactions between the filled orbitals of one subsystem and vacant orbitals of another subsystem, the natural bond orbital (NBO) calculation was performed using NBO 3.1 program implemented in the GAUSSIAN 09W package at the DFT/B3LYP level. In BFB, the hyperconjugative interaction energy was deduced from the second-order perturbation approach[22]. Delocalization of electron density between occupied Lewis-type (bond or lone pair) NBO orbitals and formally unoccupied (antibond or Rydberg) non-Lewis NBO orbitals corresponds to a stabilizing donor–acceptor interaction. The comparison between 'filled' (donors) Lewis-type NBOs and 'empty' (acceptors) non-Lewis NBOs according to second order perturbation energy values, $E(2)_{ij}$ of BFB are given in Table 4. In NBO analysis large E(2) value shows the intensive interaction between electron-donors and electron-acceptors and greater the extent of conjugation of the whole system. The electron density of conjugated single as well as double bond of benzene ring (~0.9e) clearly demonstrates strong delocalization for BFB. The strong intramolecular hyperconjugative interaction of the σ and π electrons of C–C bonding to the C–C antibonding of the ring leads to stabilization of some part of the ring as evident from

Table 4. For example, In BFB, the intramolecular hyperconjugative interaction of σ(C1-C2) → σ*(C2-C3) and π(C1-C2) → π*(C5-C6) leading to stabilization of 2.25 and 9.91 kJ/mol, respectively. The intramolecular interaction are formed by the orbital overlap between bonding and antibonding C-C and C-Br orbitals which results intramolecular charge transfer (ICT) causing stabilization of the system. These interactions are observed as increase in electron density (ED) in C–C, C–Br antibonding orbital that weakens the respective bonds. The energies for the interaction n3(Br7) → π*(C1-C2) and n3(F8) → π*(C1-C2) are 5.50 and 9.84 kJmol^{-1}, respectively clearly demonstrate the intramolecular hyperconjugative interaction between the halogen atoms and benzene ring is strong in the ground state for BFB. There occurs a strong intramolecular hyperconjugative interaction of π*(C1-C2)→ π*(C5-C6) which increases electron density that weakens the respective bond (C5-C6 = 1.3865 Å) leading to stabilization of 122.85 kJ mol^{-1}. These charge transfer interactions of BFB are responsible for pharmaceutical and biological properties. Hence the BFB structure is stabilized by these orbital interactions.

Table 3: Vibrational assignments of fundamental modes of 1,4-dibromo-2,5-difluorobenzene along with calculated IR and Raman intensities (characterized by TED) based on DFT force field calculation using B3LYP/6-311++G(d,p) method.

Sl.No.	Observed Frequencies (cm^{-1})		Calculated Frequencies (cm^{-1}) B3LYP/6-311++G(d, p)					Assignment (% of TED)
	FTIR	FT-Raman	Unscaled	Scaled	Force Constants	IR intensity[a]	Raman activity[b]	
1	3092(s)	-	3214	3089	6.649	0.00	164.33	ν CH(98)
2	3084(w)	3088(s)	3212	3087	6.638	5.63	0.00	νCH(97)
3	1624(s)	1621(w)	1622	1559	11.327	0.00	46.88	ν CC (88)
4	1562(w)	1556(s)	1612	1549	16.561	0.00	24.98	ν CC (85)
5	1452(vs)	-	1504	1445	4.907	297.64	0.00	ν CC (82)
6	1354(vs)	1352(vw)	1388	1334	9.909	39.10	0.00	ν CC (80)
7	1263(vs)	-	1308	1257	12.04	9.87	0.00	ν CC (79)
8	-	1272(ms)	1298	1247	11.05	0.00	40.51	ν CC (75)
9	-	1245(ms)	1270	1219	1.109	0.00	3.99	b CH (78)
10	1235(w)	-	1260	1210	2.039	89.53	0.00	b CH (79)
11	1205(ms)	-	1238	1190	1.769	70.94	0.00	ν CF (71), b CBr (16)
12	1156(vs)	-	1197	1151	5.740	0.00	15.33	ν CF (70) , b CH (15)
13	1042(vs)	-	1077	1035	0.660	41.50	0.00	R asymd (75), b CH (20)
14	917(w)	922(ms)	947	910	0.609	0.00	0.35	R symd (74), b CF (18)
15	865(vs)	-	890	855	2.533	107.20	0.00	ω CH (60), t R trigd (19)
16	822(w)	-	851	818	2.294	0.00	15.61	ω CH (58), t R asymd (20)
17	762(vs)	-	786	755	1.072	0.00	0.67	R trigd (70), b CBr (19)
18	-	693(vs)	701	674	2.255	0.42	0.00	ν CBr (72), b CH (18)
19	620(ms)	-	637	612	1.111	0.00	1.77	ν CBr (70), b CF (15)
20	-	542(ms)	566	543	1.464	18.10	0.00	t R trigd (57), ω CBr (19)
21	480(s)	-	483	464	1.706	0.00	7.25	t R asymd (55), ω CH (20)
22	-	441(s)	455	437	0.382	6.07	0.00	t R symd (58), ω CF (22)
23	-	377(ms)	388	372	1.028	0.00	1.06	b CBr (65), R asymd (20)
24	-	265(ms)	286	274	1.043	0.63	0.00	b CBr (64), b CH (19)
25	-	210(ms)	218	209	0.178	0.00	1.68	b CF (66), b CH (15)
26	-	202(vs)	215	207	1.324	0.00	6.26	b CF (65), R asymd (18)
27	-	190(ms)	192	184	0.382	0.00	0.91	ω CBr (54), t R trigd (17)
28	-	165(vw)	168	161	0.209	1.14	0.00	ω CBr (52), ω CH (19)
29	-	145(w)	146	140	0.222	0.06	0.00	ω CF (53), ω CH (20)
30	-	70(vw)	65	62	0.047	0.02	0.00	ω CF (52), t R trigd (18)

Abbreviations used : v-stretching; b-bending; ω-out-of-plane bending; R-ring; trigd-trigonal deformation; symd-symmetric deformation; asymd-antisymmetric deformation; t-torsion; s-strong; vs-very strong; ms-medium strong; w-weak; vw-very weak.

[a]Relative absorption intensities in km mol^{-1} and normalised with the highest peak absorbance.

[b] Relative Raman intensities in $Å^4amu^{-1}$ and normalised to 100.

Table 4: Second-order perturbation theory analysis of Fock matrix in NBO basis for 1, 4-dibromo-2,5-difluorobenzene.

Donor (i)	ED (i) (e)	Acceptor (j)	ED (j) (e)	[a]E(2) (kJ mol^{-1})	[b]E(j)–E(i) (a.u.)	[c]F (i,j) (a.u.)
σ(C1-C2)	0.99060	σ*(C1-C6)	0.01065	1.32	1.31	0.052
		σ* (C2-C3)	0.01416	2.25	1.30	0.068
π(C1-C2)	0.83693	π*(C3-C4)	0.20780	9.70	0.29	0.069
		π*(C5-C6)	0.18362	9.91	0.30	0.069
σ(C2-C3)	0.98311	σ*(C1-C2)	0.01989	2.66	1.27	0.073
		σ* (C1-Br7)	0.01414	2.34	0.82	0.056
		σ* (C4-Br10)	0.01414	2.46	0.82	0.057
π(C3-C4)	0.85239	π*(C1-C2)	0.21920	9.90	0.28	0.069
		π*(C5-C6)	0.18362	10.10	0.29	0.070
σ(C4-C5)	0.99060	σ*(C3-C4)	0.01065	1.32	1.31	0.052
		σ*(C5-C6)	0.01416	2.25	1.30	0.068
σ(C5-C6)	0.98311	σ*(C1-Br7)	0.01414	2.46	0.82	0.057
		σ*(C4-C5)	0.01989	2.66	1.27	0.073
		σ*(C4-Br10)	0.01414	2.34	0.82	0.056
π(C5-C6)	0.83340	π*(C1-C2)	0.21920	9.63	0.28	0.067
		π*(C3-C4)	0.20780	9.72	0.28	0.067
n3(Br7)	0.96450	π*(C1-C2)	0.21920	5.50	0.29	0.055
n2(F8)	0.98471	σ*(C1-C2)	0.01989	3.02	0.96	0.068
		σ* (C2-C3)	0.01416	3.13	0.97	0.070
n3(F8)	0.96200	π*(C1-C2)	0.21920	9.84	0.41	0.089
n3(Br10)	0.96450	π*(C3-C4)	0.20780	5.36	0.29	0.055
n2(F11)	0.98471	σ*(C4-C5)	0.01989	3.02	0.96	0.068
		σ*(C5-C6)	0.01416	3.13	0.97	0.070
n3(F11)	0.96200	π*(C5-C6)	0.18362	9.41	0.43	0.087
π*(C1-C2)	0.21920	π*(C5-C6)	0.18362	122.85	0.01	0.079

[a]E(2) means energy of hyperconjugative interactions.

[b]Energy difference between donor and acceptor i and j NBO orbitals.

[c]F(i,j) is the Fock matrix element between i and j NBO orbitals.

Electrostatic potential, total electron density and molecular electrostatic potential

For predicting sites and relative reactivities towards electrophilic attack, and in studies of biological recognition and hydrogen bonding interactions, the electrostatic potential has been utlized[23]. To predict reactive sites for electrophilic and nucleophilic attack for the investigated molecule, the MEP at the B3LYP/6-311++G(d,p) optimized geometry is calculated. In the present investigation, the electrostatic potential (ESP), electron density (ED) and the molecular electrostatic potential (MEP) map figures for BFB are shown in Fig. 4. The ED plots for BFB show a uniform distribution. However, it can be seen from the ESP figures, that the negative ESP is localized more over the bromine and fluorine atoms and is reflected as a yellowish blob, the positive ESP is localized on the rest of the molecule. This result is expected, because ESP correlates with electro negativity and partial charges. The negative (red and yellow) regions of the MEP are related to electrophilic reactivity and the positive (blue) regions to nucleophilic reactivity, as shown in Fig. 4. Generally, the potential energy increases from red < orange < yellow < green < blue. In the present study, the MEP map shows that the negative potential sites are on halogen atoms (Red) and the positive potential sites are around the hydrogen

atoms of the benzene ring (Blue). From these results, one can say that the H atoms indicate the strongest attraction and halogen atoms indicate the strongest repulsion. These sites provide information about the region of intermolecular interactions for the title compound. Thus, the results indicate that the BFB will be the most reactive site for both electrophilic and nucleophilic attack.

CONCLUSION

The optimized geometries, harmonic vibrational wavenumbers and intensities of vibrational bands of 1,4-dibromo-2,5-difluorobenzene have been determined using DFT-B3LYP with 6-311++G(d,p) level calculation. The normal modes of BFB have been studied by FTIR and FT-Raman spectroscopies on the basis of C_{2h} point group symmetry. The TED calculation regarding the normal modes of vibration provides a strong support for the frequency assignment. The NBO analysis reveals hyper conjugative interaction, ICT and stabilization of the molecule. The molecular orbitals, MESP surface drawn and the lowering of HOMO-LUMO band gap may lead to the understanding of properties and chemical activity of the molecule. So the results will be of assistance in the quest of the experimental and theoretical evidence for 1,4-dibromo-2,5-difluorobenzene in reaction intermediates, pharmaceuticals and polymer science.

REFERENCES

1. Halliwell B, Gutteridge JMC, Free Radicals in Biology and Medicine, 2nd edition, Oxford University Press, Oxford, 1989.
2. Gugumus F, Oxidation Inhibition in Organic Materials, vol. 1, CRC Press, BocaRaton, 1990.
3. Mahadevan D, Periandy S, Karabacak M, Ramalingam S, FT-IR and FT-Raman, UV spectroscopic investigation of 1-bromo-3-fluorobenzene using DFT (B3LYP, B3PW91 and MPW91PW91) calculations, Spectrochim. Acta, 82A, 2011, 481-492.
4. Kolesnikova IN, Dorofeeva OV, Karasev NM, Oberhammer H, Shishkov IF, Molecular structure and conformation of 1,3,5-tris(trifluoromethyl)-benzene as studied by gas-phase electron diffraction and quantum chemical calculations, J. Mol. Struct., 1074, 2014, 196–200.
5. Hosseinzadeh R, Moosavi-Movahedi AA, Human hemoglobin structural and functional alterations and heme degradation upon interaction with benzene: A spectroscopic study, Spectrochim. Acta, 157A, 2016, 41–49.
6. Vennila P, Govindaraju M, Venkatesh G, Kamal C, Armaković SJ, A complete computational and spectroscopic study of 2-bromo-1, 4-dichlorobenzene – A frequently used benzene derivative, J. Mol. Struct., 1151 (2018) 245– 255.
7. Frisch MJ, Trucks GW, Schlegel HB, Scuseria GE, Robb MA, Cheeseman JR, Scalmani G, Barone V, Mennucci B, Petersson GA, Nakatsuji H, Caricato M, Li X, Hratchian HP, Izmaylov AF, Bloino J, Zheng G, Sonnenberg JL, Hada M, Ehara M, Toyota K, Fukuda R, Hasegawa J, Ishida M, Nakajima T, Honda Y, Kitao O, Nakai H, Vreven T, Montgomery JA, Peralta JE, Ogliaro F, Bearpark M, Heyd JJ, Brothers E, Kudin KN, Staroverov VN, Kobayashi R, Normand J, Raghavachari K, Rendell A, Burant JC, Iyengar SS, Tomasi J, Cossi M, Rega N, Millam JM, Klene M, Knox JE, Cross JB, Bakken V, Adamo C, Jaramillo J, Gomperts R, Stratmann RE, Yazyev O, Austin AJ, Cammi R, Pomelli C, Ochterski JW, Martin RL, Morokuma K, Zakrzewski VG, Voth GA, Salvador P, Dannenberg JJ, Dapprich S, Daniels AD, Farkas O, Foresman JB, Ortiz JV, Cioslowski J, Fox DJ, GAUSSIAN 09, Revision A.02, Gaussian Inc, Wallingford CT, 2009.
8. Becke AD, Density-functional thermochemistry. III. The role of exact exchange, J. Chem. Phys. 98, 1993, 5648–5652.
9. Lee C, Yang W, Parr RR, Development of the Colle-Salvetti correlation-energy formula into a functional of the electron density, Phys. Rev. B 37, 1988, 785–789.
10. MOLVIB (V.7.0): Calculation of Harmonic Force Fields and Vibrational Modes of Molecules, QCPE Program No. 807, 2002.
11. Schultz G, Kolonits M, Hargittai I, Portalone G, Domenicano A, Molecular structure and ring distortions of p-dibromobenzene as determined by electron diffraction, J. Mol. Struct., 176, 1988, 71–80.
12. Kirchner MT, Bläser D, Boese R, Thakur TS, Desiraju GR, 1,3-Difluorobenzene, Acta Cryst., E65, 2009, o2668-o2669.
13. Zhang R, Du B, Sun G, Sun Y, Experimental and theoretical studies on o-, m- and p-chlorobenzylideneaminoantipyrines, Spectrochim. Acta, 75A, 2010, 1115–1124.
14. Jeyavijayan S, Molecular structure, spectroscopic (FTIR, FT-Raman, 13C and 1H NMR, UV), polarizability and first-order hyperpolarizability, HOMO–LUMO analysis of 2,4-difluoroacetophenone, Spectrochim. Acta, 136A, 2015, 553–566.
15. Young DC, Computational Chemistry: A Practical Guide for Applying Techniques to Real World Problems (Electronic), John Wiley & Sons Ltd., New York, 2001.
16. Gobinath E, Jeyavijayan S, John Xavier R, Spectroscopic investigations, DFT computations and other molecular properties of 2,4dimethylbenzoicacid, Indian J. Pure & Appl. Phys., 55, 2017, 541-550.
17. Jeyavijayan S, Molecular structure, vibrational spectra, NBO analysis, first hyperpolarizability, and HOMO–LUMO studies of 2-amino-4- hydroxypyrimidine by density functional method, J. Mol. Struct., 1085, 2015, 137–146.
18. Arjunan V, Saravanan I, X Ravindran P, Mohan S, Structural, vibrational and DFT studies on 2-chloro-1H-isoindole-1,3(2H)-dione and 2-methyl-1H-isoindole-1,3(2H)-dione, Spectrochim. Acta, 74A, 2009, 642-649.
19. Socrates G, Infrared and Raman Characteristic Group Frequencies – Tables and Charts, third ed., Wiley, Chichester, 2001.
20. Tocon IL, Becucci M, Pietraperzia G, Castellucci E, Otero JC, Vibrational spectrum of 4-fluoraniline, J. Mol. Struct., 565, 2001, 421-425.
21. Karabacak M, Kose E, Kurt M, FT-Raman, FT-IR spectra and DFT calculations on monomeric and dimeric structures of 5-fluoro- and 5-chloro-salicylic acid, J. Raman Spectrosc., 41, 2010, 1085-1097.
22. Choo J, Kim S, Joo H, Kwon Y, Molecular structures of (trifluoromethyl)iodine dihalides CF_3IX_2 (X=F, Cl): ab initio and DFT calculations, J. Mol. Struct. (Theochem.) 587, 2002, 1-8.
23. Murray JS, Sen K, Molecular Electrostatic Potentials, Concepts and applications, Elsevier, Amsterdam, 1996, pp. 7–624.

Source of Support: Nil, **Conflict of Interest:** None.